INTERNATIONAL JOURNAL OF INTEGRATED ENGINEERING
ISSN: 2229-838X e-ISSN: 2600-7916

IJIE

Vol. 16 No. 5 (2024) 275-282
https://publisher.uthm.edu.my/ojs/index.php/ijie

# Early Detection and Quantitative Analysis of Skin Cancer Using THz Metamaterial Biosensor

**Suhail Asghar Qureshi[1], Zuhairiah Zainal Abidin[1]*, Muhammad Ramlee Kamarudin[1], Nurul Bashirah Ghazali[2]**

[1] *Advanced Telecommunication Research Center (ATRC), Faculty of Electrical and Electronic Engineering, Universiti Tun Hussein Onn Malaysia (UTHM), Batu Pahat, Johor, MALAYSIA*

[2] *EVIS, 81, Jalan Maarof, Bangsar, 59000, Kuala Lumpur, Wilayah Persekutuan Kuala Lumpur, MALAYSIA*

*Corresponding Author: zuhairia@uthm.edu.my
DOI: https://doi.org/10.30880/ijie.2024.16.05.021

**Article Info**

Received: 17 January 2024
Accepted: 21 June 2024
Available online: 12 August 2024

**Keywords**

THz, cancer, metamaterial, sensor

**Abstract**

Terahertz imaging offers significant potential for the early detection of skin cancer. This study introduces a metamaterial unit cell designed to operate in the terahertz (THz) band for non-invasive contact-based skin cancer detection. The sensor relies exclusively on the reflection coefficient response, providing high sensitivity to subtle changes in tissue properties without requiring complex signal processing. This simplicity may result in a cost-effective and straightforward implementation for early cancer detection. Simulations were conducted using 3D models representing various skin types, including normal skin, basal cell carcinoma (BCC), and melanoma. The dielectric characteristics of the samples were determined using the Double Debye model. The simulations revealed that the metamaterial design exhibited double negative material properties at a specific frequency of 1.15 THz. Upon skin contact and detection of malignancy, the reflection coefficient showed a shift toward lower frequencies. Notably, the melanoma sample exhibited the most significant shift, indicating a more severe form of cancer compared to BCC. Furthermore, it was observed that the difference in resonance frequencies between normal and malignant skin increased with the thickness of the sample. The sensor demonstrated high sensitivity in detecting cancer thickness, with a sensitivity of 9.25 GHz/μm for basal cell carcinoma (BCC) and 10.2 GHz/μm for melanoma. Furthermore, linear regression analysis revealed a robust correlation between the resonance frequency and the variation in cancer thickness, with R2 values of 0.9948 and 0.9947 for BCC and melanoma, respectively. These findings underscore the sensor's ability to detect skin cancer at its earliest stages, regardless of its severity.

## 1. Introduction

Modern lifestyles have increased persons' vulnerability to serious illnesses, demanding early diagnosis. Cancer is a significant health issue in Malaysia, with more than 200 different forms. Regrettably, more than 50% of patients are diagnosed at the advanced stage [1]. The delay in treatment is associated with both expensive expenses and demanding therapeutic interventions [2]. Skin cancer, which is caused by continuous exposure to ultraviolet (UV) radiation and is characterised by an abnormal growth of skin cells, can be classified into three main categories: basal cell carcinoma (BCC), squamous cell carcinoma (SCC), and cutaneous malignant melanoma (CMM) [3]. A

conventional diagnostic method consists of performing a biopsy, which requires using anaesthesia to numb the skin and surgically removing a potentially abnormal tissue sample, which is then subjected to laboratory analysis [4]. Nevertheless, this approach is invasive and requires a significant amount of time.

Within the field of Systems Biology, researchers have recently put forth several mechanistic models aimed at comprehending and controlling the biochemical and biophysical elements of skin cancer [5]. In contrast, biosensors, which are small, easy to use, and can be carried around, provide a practical method for detecting skin cancer. Biosensors provide convenient and effective real-time monitoring without necessitating the use of labelling. Terahertz (THz) frequency-based biosensors have made significant advancements in the development of advanced sensing technology. The frequency range from 0.1 THz to 10 THz offers photons with low energy levels and strong penetrating capabilities [6]. Furthermore, this frequency spectrum corresponds to the vibrational energy levels seen in several biomacromolecules. The distinctive characteristics of THz waves have created opportunities for in-vivo medical imaging and diagnostics. However, the direct detection of trace-level chemicals at THz frequencies is difficult because water molecules have a significant tendency to absorb these frequencies [6]. To overcome this obstacle, one can utilise metamaterials (MMs) to enhance the electromagnetic field [7], [8].

It is crucial to acknowledge that THz frequencies cause no harm to living cells or the human body because of their low energy levels. Moreover, the THz band contains the rotational and vibrational energy levels of several polar chemicals and macromolecules found in biological systems. The ability to analyse and identify biological tissues can be enhanced using this characteristic [9]. Tumours typically exhibit more water content in comparison to healthy tissues, leading to substantial absorption of THz waves. As a result, tumours can be identified by analysing their unique THz absorption spectra [10]. Several recent studies have presented a variety of sensors based on metamaterials to detect cancer [11-14]. An example is the Terahertz (THz) Metamaterial (MM) suggested in reference [15], which achieves a 99% absorption rate at a frequency of 3.71 THz. Reference [16] proposed an alternative sensor consisting of two hexagonal gold layers stacked in loops, which achieved a remarkable absorption rate of 99.9% at a frequency of 3.15 THz. In [17], a very sensitive triple-band biosensor based on metamaterials was presented for detecting different forms of cancer. The sensor employed a polyimide dielectric layer with a gold patch and full grounding on its lower surface. The analyte sample filled the metallic patch, resulting in numerous resonances. In addition, a new technique for detecting skin cancer was suggested in reference [18], which utilises a semiconductor film and water-based terahertz MM to achieve increased sensitivity. The technique of utilising terahertz pulse imaging in a reflection geometry was applied to accurately detect and identify skin-related cancers. Azizi et al. [19] proposed a simplified method for early diagnosis of skin cancer by integrating split ring resonators (SRRs) into the central region of the T-shaped prototype line. The SRR enhanced the strength of the electric field, but the gaps mostly contributed to the capacitance and clustering of the electric field.

However, most of the past studies have concentrated on predetermined sample sizes or consistent sample volumes, which frequently exhibit variations in real-world scenarios. Our paper presents a novel resonator that utilises THz metamaterials to detect the two prevalent types of skin cancer at an early stage. We analyse the characteristics of basal cell carcinoma (BCC) and melanoma by utilising second-order Debye dielectric properties. Crucially, our methodology considers both the thickness and location of the tumour, which helps in accurately identifying where the tumour is and assessing the severity of the cancer. This metamaterial sensor utilises direct contact with the sample to minimise reflections and impedance mismatches between the sensor and the skin. Our metamaterial sensor operates in the THz frequency range and can detect skin cancer during its initial phases. This new sensor is expected to have substantial lateral sensitivity in the THz frequency range, enabling it to distinguish between healthy and malignant skin properties.

## 2. Method

The sensor design proposed is shown in Figure 1, which was modelled and simulated using the 3D EM analysis software package, CST Microwave Studio Suite. The design is based on a square-shaped slot with two square patches inside it. As seen in the layered view (Figure 1 (b)), the sensor has a dual-layer construction that incorporates gold and polyimide materials with a unit cell area is 0.22 $mm^2$. Gold is used as a metallic part and polyimide with a dielectric constant (ε) of 3.5 is used as the substrate part. The thickness of the polyimide substrate, (h) and gold patch, (t), is 15 µm and 1 µm, respectively. The dimensions of the unit cell are given in Table 1. Figure 2 shows the reflection coefficient ($S_{11}$) response of the design. The resonance of the design is realised at 1150 GHz with a magnitude of -15 dB. This technique allows for the non-invasive detection of malignant skin cells with just one port, increasing sensitivity in the detection of changes in the reflection coefficient without the need for a second port. It is assumed that the unit cell acts as a metamaterial if it represents negative permeability (µ) and negative permittivity (ε). The permittivity and permeability of the unit cell were extracted using the Numerical Robust Method (NRM) [20]. As illustrated in Figure 3, the constitutive parameters of MM are viewed as negative at the resonance frequency of 1150 GHz, hence the unit cell shows double negative MM characteristics.

Int. Journal of Integrated Engineering Vol. 16 No. 5 (2024) p. 275-282

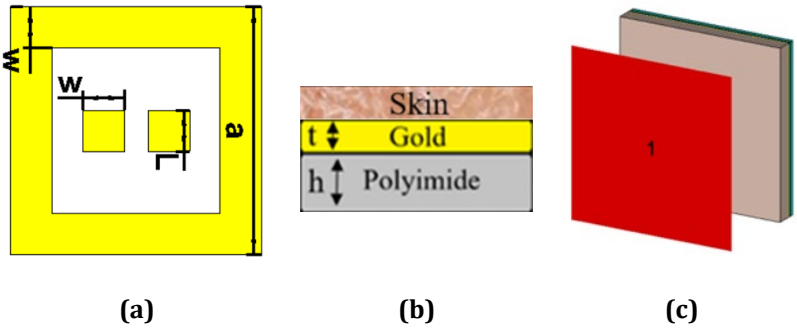


**Fig. 1** *Metamaterial design and simulation setup (a) front view of a unit cell; (b) layered view: top with skin sample; (c) the simulation setup*

**Table 1** *Dimensions of the design*

| Label | Value (μm) |
|---|---|
| W | 25 |
| L | 25 |
| a | 150 |
| t | 1 |
| h | 15 |

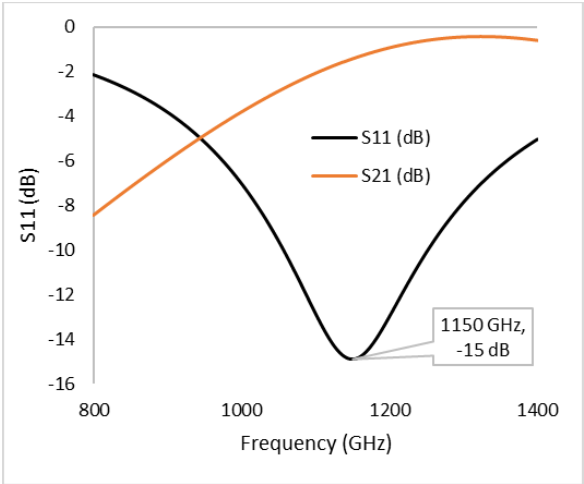


**Fig. 2** *Resonance frequency of the MM design*

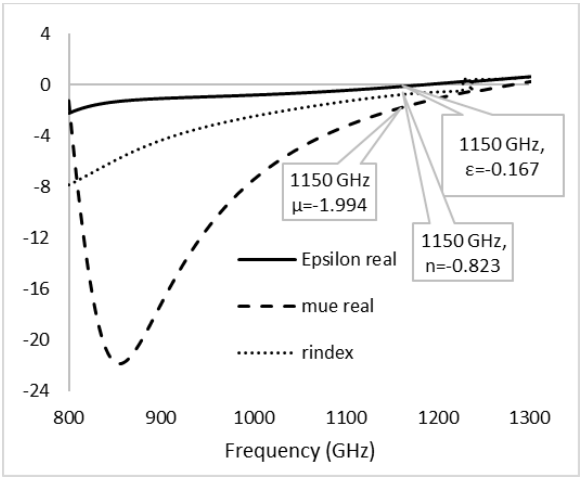


**Fig. 3** *Extracted constitutive parameters of the designed unit cell*

Subsequently, the surface of the metamaterial is investigated along with its interaction with the skin sample. The electric and magnetic field distributions, with and without a skin sample, are illustrated in Figures 4 and 5, respectively. In Figure 4(a), the electric field strength is measured to be 3.8 V/m when there is no contact between the skin and the electric field. Conversely, Figure 4(b) demonstrates that the electric field intensity decreases to 3.13105 V/m upon contact with the skin. The primary regions where the electric field distributions are concentrated are the upper and lower gaps between the two square patches of the sensor. Figure 5(a) displays the H-field distributions, with the square patches' boundaries exhibiting the most strong magnetic field, measuring approximately 1070 A/m. When the skin makes contact with the sensor's surface, the H-field decreases to a maximum value of 969 A/m.

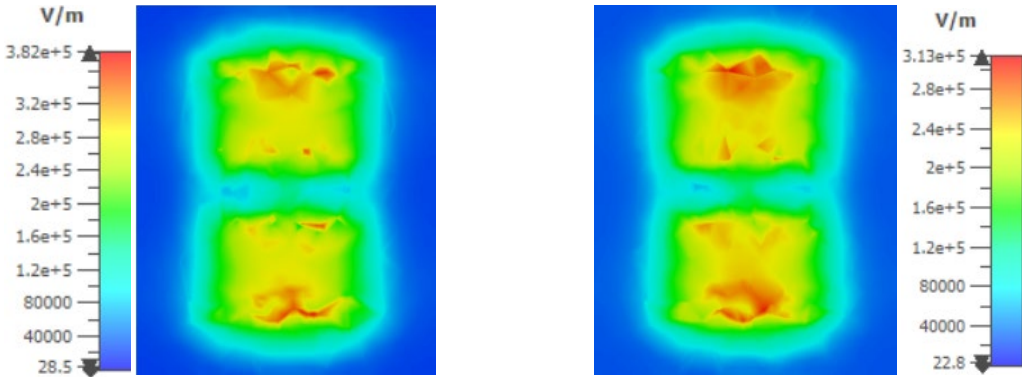


**(a)** **(b)**

**Fig. 4** *E-field distributions (a) without skin; (b) with skin*

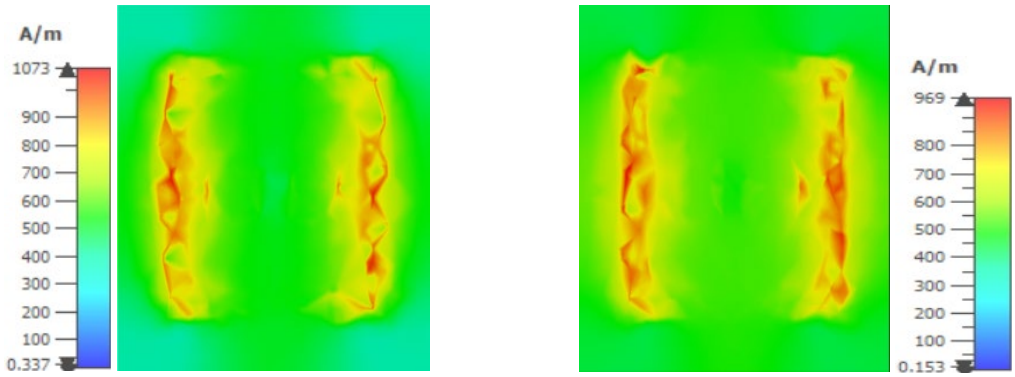


**(a)** **(b)**

**Fig. 5** *H-field distributions (a) Without skin; (b) With skin*

The designing of the sensor of high sensitivity which can identify various skin cancer cell types (such as BCC and CMM) at various thicknesses of skin tumours is the main contribution of this study. Near field electromagnetic (EM) waves are essential to the system's operation. A portion of the signal travels through the skin as a result of the produced THz waves passing through the sensor design, with the remaining power being reflected via the design. Resonance frequency and amplitude of the reflected signal provide important information about the extent of tumour spreading through skin. This study examines the fluctuation in resonance frequency in the case of malignant cells, namely BCC and CMM, in a normal skin sample.

## 3. Skin Cancer Detection

Complicated conductivity or permittivity measurements must be used to correctly depict the properties of any substance in EM simulations [21]. The double Debye model may be used to predict human skin's dielectric behaviour in the THz frequency range, according to [22]. The Double Debye model is based on two relaxation values that illustrate accurately how an applied electric field affects water molecules [23]. This study focuses on the phenomenon of the interaction between water molecules in the skin and terahertz radiation. The Double Debye model, as described in equation (1), may be used to characterize the complex dielectric variables in the THz band.

Int. Journal of Integrated Engineering Vol. 16 No. 5 (2024) p. 275-282

$$\varepsilon(\omega) = \varepsilon_\infty + \frac{\varepsilon_s - \varepsilon_2}{1 + i\omega\tau_1} + \frac{\varepsilon_2 - \varepsilon_\infty}{1 + i\omega\tau_2} \quad (1)$$

In this case, $\varepsilon_s$ denotes static permittivity, $\varepsilon_\infty$ denotes the permittivity at highest frequency, $\varepsilon_2$ denotes the intermediate frequency limit, $\tau_1$ denotes slow relaxation frequency, and $\tau_2$ denotes rapid relaxation frequency [18]. Pickwell's [24] well-known Double Debye features of BCC is employed in this analysis. While the criteria for normal skin were taken from [21], the parameters for melanoma were taken from [25]. The Double Debye parameters for normal skin, BCC, and melanoma that were simulated are summarized in Table 2.

**Table 2** *Double Debye parameters of normal skin, BCC and melanoma*

| Sample | $\varepsilon_\infty$ | $\varepsilon_s$ | $\varepsilon_2$ | $\tau_1$(PS) | $\tau_2$ (ps) |
|---|---|---|---|---|---|
| Normal Skin | 3.4 | 25 | 5 | 7 | 1 |
| BCC | 4.2 | 40 | 6.2 | 10 | 1 |
| Melanoma | 4.3 | 58 | 4.6 | 5 | 0.49 |

3D portrayal in Figure 6 offers a comprehensive depiction of many cancer kinds, revealing the disease's concealed growth beneath the skin, particularly in its early stages when symptoms are not readily noticeable. This work proposes a skin model with a concealed layer of cancer at various levels to address this challenge. After that, simulations are run, with a focus on various cancer thicknesses, to help with early cancer identification. The outcomes of the simulation for the emergence of basal cell carcinoma (BCC) are shown in Figure 7. Situations without BCC, which show normal skin of the same thickness, are illustrated by dotted lines, whereas findings for BCC are shown by solid lines. A comparative analysis is carried out to investigate the distinctions between skin cancer and healthy skin. Notably, as the thickness of the BCC layer increases, the resonance shifts towards lower frequencies. This is illustrated by a frequency shift that occurs as the BCC thickness changes from 10 μm to 50 μm, from 914 GHz to 579 GHz.

When melanoma is present, Figure 8 shows a more noticeable shift in resonance frequency than when BCC is present. The graphic uses a consistent depiction, with dotted lines representing normal skin results and solid lines indicating melanoma discoveries. When melanoma thickness increases from 10 μm to 50 μm, resonance shifts to lower frequencies from 900 GHz to 558 GHz. The greater alteration is attributed to melanoma's disruptive effect on the skin's dielectric properties. Double Debye analysis immediately observes magnified resonance shifts due to increased dielectric disturbances caused by melanoma. Furthermore, melanoma is associated with a permanent change in resonant frequency that is reminiscent of basal cell carcinoma (BCC). As sample thickness grows, the frequency resonance decreases more sharply, demonstrating our sensor's capacity to precisely identify and quantify the extent of skin cancer using fine-grained THz imaging.

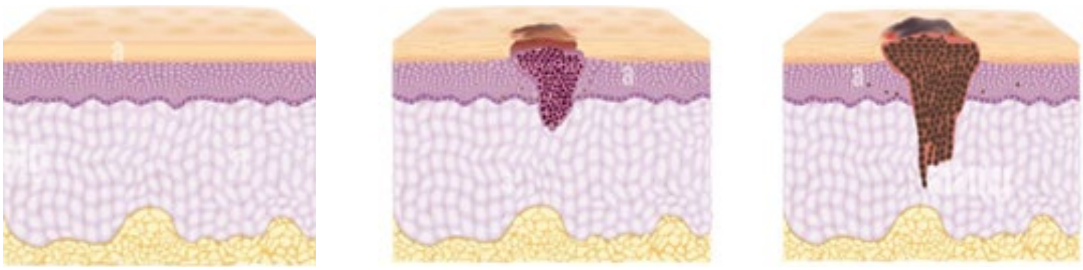

**(a)** **(b)** **(c)**

**Fig. 6** *Samples considered in this study (a) Normal skin; (b) BCC; (c) Melanoma* [26]

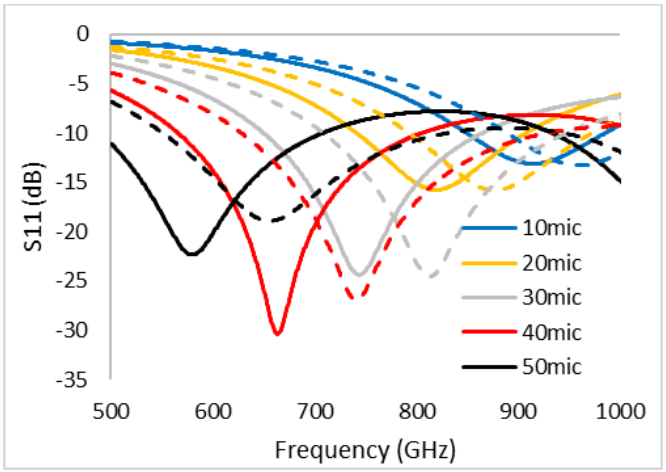


**Fig. 7** *$S_{11}$ at* different *thicknesses of BCC (___) and normal skin (---)*

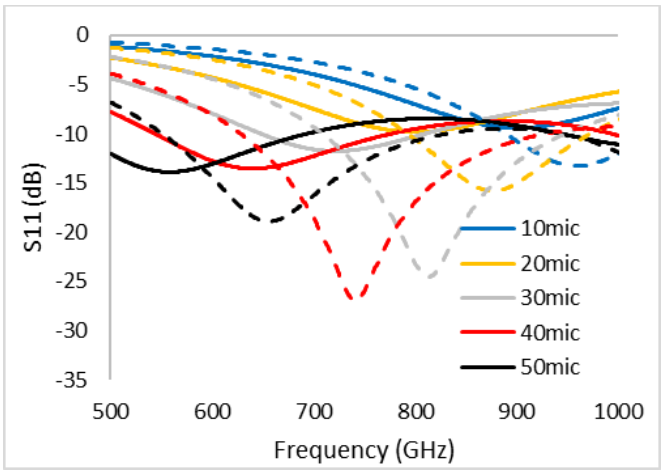


**Fig. 8** *$S_{11}$ at* different *thicknesses of melanoma (__) and normal skin (---)*

## 4. Analysis and Discussion

This part does a sensitivity study of the sensor. Analysing the sensitivity of the MM sensor is crucial to determining its ability to detect malignant cells in the skin. The sensitivity was estimated using equation (2).

$$S = \Delta f / \Delta t \tag{2}$$

The sensor's sensitivity (S) is characterized by the ratio of the shift in frequency (Δf) to the change in thickness (Δt) of the malignant cell, given as S = Δf/Δt. In our investigation, the sensor showed a sensitivity of 8.365 GHz per micron for basal cell carcinoma (BCC) and 8.558 GHz per micron for melanoma. Compared to BCC, the sensor notably shows a greater intensity in melanoma detection. Even with a maximum malignant cell thickness of 25 µm (depending on real-world variances), the sensor can still identify skin cancer samples with higher thicknesses.

Resonance frequency was treated as the independent variable and skin cancer thickness as the dependent variable in a linear regression analysis used to further analyse the data. Practitioners can estimate the depth of skin cancer growth with the use of this analytical method. With an $R^2$ value of 0.9987, Figure 9 shows how well the linear regression model predicts BCC thickness. Similarly, the prediction performance of the proposed sensor for melanoma thickness, provides an $R^2$ value of 0.9981. The exceptionally high $R^2$ values highlight the sensor's remarkable efficacy in early cancer detection by confirming the linearity of the resonance shift concerning variations in the thickness of malignant cells.

Int. Journal of Integrated Engineering Vol. 16 No. 5 (2024) p. 275-282

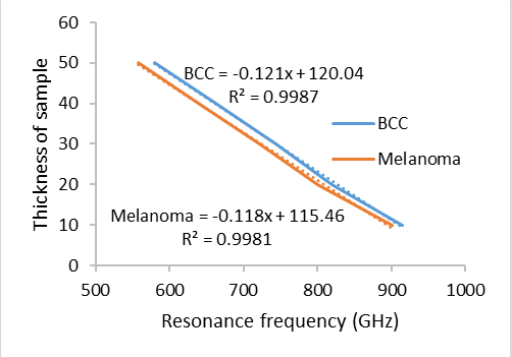


**Fig. 9** *Linear regression applied to the results obtained from the sensor*

## 5. Conclusion

In summary, we present a novel miniaturised biosensor that operates within the THz frequency range and exhibits significant promise for the early detection of skin cancer. To better understand the use of THz imaging for detecting skin cancer, we simulate how THz radiation interacts with both cancerous and healthy skin tissues. The sensor's high sensitivity to polar molecules, particularly water, makes it highly useful for cancer detection, considering the association between elevated amounts of water molecules in the skin and the progression of cancer. The proposed sensor enables the non-intrusive evaluation of skin samples that come into contact with it, thanks to its unique single-port configuration. The objective of this study was to examine the differences between healthy and malignant skin in two common kinds of skin cancer: melanoma and basal cell carcinoma. The sensor demonstrates a linear response to changes in resonance frequency corresponding to variations in sample thickness, implying its potential for measuring thicknesses beyond the scope of this investigation. The utilisation of the linear regression method, as a reliable analytical instrument, proves advantageous in evaluating the severity of cancer. The sensor, which has been specifically built, evaluates the varying thicknesses of cancerous cells and exhibits exceptional efficacy in assessing the range of cancer severity, encompassing both mild and more serious conditions. The results emphasise the sensor's capacity to transform skin cancer monitoring and early detection, creating a significant opportunity to enhance patient outcomes and medical analysis.

## Acknowledgement

This research was supported by Universiti Tun Hussein Onn Malaysia (UTHM) through TIER 1 (Vot Q447).

## Conflict of Interest

Authors declare that there is no conflict of interest regarding the publication of the paper.

## Author Contribution

*The authors confirm contribution to the paper as follows:* ***study conception and design:*** *Suhail Asghar Qureshi;* ***data collection:*** *Zuhariah Zainal Abidin;* ***preparation of the manuscript:*** *Suhail Asghar Qureshi, Zuhariah Zainal Abidin;* ***technical assistance:*** *Muhammad Ramlee Kamarudin, Nurul Bashirah Ghazali. All authors reviewed the results and approved the final version of the manuscript.*

## References

This guide contains examples of common types of APA Style references. Section numbers indicate where to find the examples in the Publication Manual of the American Psychological Association (7th ed.).

[1] Ministry of Health Malaysia. (2019). Ten most common cancers in Malaysia - ministry of health. https://www.moh.gov.my/moh/resources/Penerbitan/Laporan/Umum/2012-2016%20(MNCRR)/Summary_MNCR_2012-2016_-_06112020.pdf.

[2] Chandra, A., Pius, C., Nabeel, M., Nair, M., Vishwanatha, J. K., Ahmad, S., & Basha, R. (2019). Ovarian cancer: Current status and strategies for improving therapeutic outcomes. *Cancer Medicine*, *8*(16), 7018–7031. https://doi.org/10.1002/cam4.2560.

[3] de Gruijl, F. R. (1999). Skin cancer and solar UV radiation. *European Journal of Cancer*, *35*(14), 2003–2009. https://doi.org/10.1016/S0959-8049(99)00283-X

[4] Privalle, A., Havighurst, T., Kim, K., Bennett, D. D., & Xu, Y. G. (2020). Number of skin biopsies needed per malignancy: Comparing the use of skin biopsies among dermatologists and nondermatologist clinicians. *Journal of the American Academy of Dermatology*, *82*(1), 110–116. https://doi.org/10.1016/j.jaad.2019.08.012.

[5] Kundal, S., & Khandelwal, A. (2023). Multiplexed Hybrid Plasmonic Ring Resonator Sensor for Label Free Biosensing Applications. *Sensing and Imaging*, *24*(1), 16. https://doi.org/10.1007/s11220-023-00422-9
[6] Xie, D., Li, D., Hu, F., Wang, Z., Zhang, L., Jiang, M., & Wang, Y. (2023). Terahertz Metamaterial Biosensor With Double Resonant Frequencies for Specific Detection of Early-Stage Hepatocellular Carcinoma. *IEEE Sensors Journal*, *23*(2), 1124–1131. https://doi.org/10.1109/JSEN.2022.3225344.
[7] Xu, W., Xie, L., Zhu, J., Tang, L., Singh, R., Wang, C., Ma, Y., Chen, H.-T., & Ying, Y. (2019). Terahertz biosensing with a graphene-metamaterial heterostructure platform. *Carbon*, *141*, 247–252. https://doi.org/10.1016/j.carbon.2018.09.050
[8] Zeng, H., Lan, F., Zhang, Y., Liang, S., Wang, L., Yin, J., Song, T., Wang, L., Zhang, T., Shi, Z., Yang, Z., & Mazumder, P. (2020). Broadband terahertz reconfigurable metasurface based on 1-bit asymmetric coding metamaterial. *Optics Communications*, *458*, 124770. https://doi.org/10.1016/j.optcom.2019.124770
[9] Grigorev, R., Kuzikova, A., Demchenko, P., Senyuk, A., Svechkova, A., Khamid, A., Zakharenko, A., & Khodzitskiy, M. (2019). Investigation of Fresh Gastric Normal and Cancer Tissues Using Terahertz Time-Domain Spectroscopy. *Materials*, *13*(1), 85. https://doi.org/10.3390/ma13010085
[10] Li, D., Hu, F., Zhang, H., Chen, Z., Huang, G., Tang, F., Lin, S., Zou, Y., & Zhou, Y. (2021). Identification of Early-Stage Cervical Cancer Tissue Using Metamaterial Terahertz Biosensor With Two Resonant Absorption Frequencies. *IEEE Journal of Selected Topics in Quantum Electronics*, *27*(4), 1–7. https://doi.org/10.1109/JSTQE.2021.3058163
[11] Tabatabaeian, Z. S. (2022). Developing THz metasurface with array rectangular slot with High Q-factor for early skin cancer detection. *Optik*, *264*, 169400. https://doi.org/10.1016/j.ijleo.2022.169400
[12] Gezimati, M., & Singh, G. (2023). Terahertz Imaging and Sensing for Healthcare: Current Status and Future Perspectives. *IEEE Access*, *11*, 18590–18619. https://doi.org/10.1109/ACCESS.2023.3247196
[13] Toolabi, M., Khatir, M., Naser-Moghadasi, M., & Amiri, N. (2023). Vivaldi antenna for early cancer detection based on THz spectroscopy: Comparison between response of breast and skin cancer. *Optik*, *273*, 170440.
[14] Kumar, M., Goel, S., Rajawat, A., & Gupta, S. H. (2020). Design of optical antenna operating at Terahertz frequency for In-Vivo cancer detection. *Optik*, *216*, 164910. https://doi.org/10.1016/j.ijleo.2020.164910
[15] Banerjee, S., Dutta, P., Jha, A. V., Appasani, B., & Khan, M. S. (2022). A Biomedical Sensor for Detection of Cancer Cells Based on Terahertz Metamaterial Absorber. *IEEE Sensors Letters*, *6*(6), 1–4. https://doi.org/10.1109/LSENS.2022.3178918
[16] Azab, M. Y., Hameed, M. F. O., Nasr, A. M., & Obayya, S. S. A. (2021). Highly Sensitive Metamaterial Biosensor for Cancer Early Detection. *IEEE Sensors Journal*, *21*(6), 7748–7755. https://doi.org/10.1109/JSEN.2021.3051075
[17] Elhelw, A. R., Ibrahim, M. S. S., Rashed, A. N. Z., Mohamed, A. E.-N. A., Hameed, M. F. O., & Obayya, S. S. A. (2023). Highly Sensitive Triple-band THz Metamaterial Biosensor for Cancer Cell Detection. *IEEE Photonics Journal*, *PP*, 1–14. https://doi.org/10.1109/JPHOT.2023.3330930
[18] Keshavarz, A., & Vafapour, Z. (2019). Water-Based Terahertz Metamaterial for Skin Cancer Detection Application. *IEEE Sensors Journal*, *19*(4), 1519–1524. https://doi.org/10.1109/JSEN.2018.2882363
[19] Azizi, S., Nouri-Novin, S., Seyedsharbaty, M. M., & Zarrabi, F. B. (2018). Early skin cancer detection sensor based on photonic band gap and graphene load at terahertz regime. *Optical and Quantum Electronics*, *50*(6), 230. https://doi.org/10.1007/s11082-018-1496-y
[20] Chen, X., Grzegorczyk, T. M., Wu, B.-I., Pacheco, J., & Kong, J. A. (2004). Robust method to retrieve the constitutive effective parameters of metamaterials. *Physical Review E*, *70*(1), 016608. https://doi.org/10.1103/PhysRevE.70.016608
[21] Chan, K. Y., & Ramer, R. (2018). Novel concept of detecting basal cell carcinoma in skin tissue using a continuous-wave millimeter-wave rectangular glass filled probe. *Medical Devices: Evidence and Research*, *Volume 11*, 275–285. https://doi.org/10.2147/MDER.S168338
[22] Truong, B. C. Q., Hoang Duong Tuan, Ha Hoang Kha, & Nguyen, H. T. (2013). Debye Parameter Extraction for Characterizing Interaction of Terahertz Radiation With Human Skin Tissue. *IEEE Transactions on Biomedical Engineering*, *60*(6), 1528–1537. https://doi.org/10.1109/TBME.2013.2237908
[23] Truong, B. C. Q., Tuan, H. D., Fitzgerald, A. J., Wallace, V. P., & Nguyen, H. T. (2014). High correlation of double Debye model parameters in skin cancer detection. *2014 36th Annual International Conference of the IEEE Engineering in Medicine and Biology Society*, 718–721. https://doi.org/10.1109/EMBC.2014.6943691
[24] Pickwell, E., Fitzgerald, A. J., Cole, B. E., Taday, P. F., Pye, R. J., Ha, T., Pepper, M., & Wallace, V. P. (2005). Simulating the response of terahertz radiation to basal cell carcinoma using ex vivo spectroscopy measurements. *Journal of Biomedical Optics*, *10*(6), 064021. https://doi.org/10.1117/1.2137667
[25] Zhang, R., Yang, K., Yang, B., AbuAli, N. A., Hayajneh, M., Philpott, M., Abbasi, Q. H., & Alomainy, A. (2019). Dielectric and Double Debye Parameters of Artificial Normal Skin and Melanoma. *Journal of Infrared, Millimeter, and Terahertz Waves*, *40*(6), 657–672. https://doi.org/10.1007/s10762-019-00597-x
[26] Siritam, S. (2017). Type of Skin Cancer in 3D vector style. https://www.alamy.com/stock-image-type-of-skin-cancer-in-3d-vector-style-160366976.html